Evolution of the electronic orbital alignment in metal-atom–rare-gas fractional collisions

T. H. Wong and P. D. Kleiber
Department of Physics and Astronomy, The University of Iowa, Iowa City, Iowa 52242
(Received 9 June 1997)

We have developed an analytic model within the ''orbital-locking and -following'' approximation to explain the observed polarization spectrum in the metal-atom–rare-gas fractional collision experiments of Olsgaard and co-workers [Phys. Rev. A **48**, 1987 (1993)]. We obtain an expression for the observed polarization spectrum that can be interpreted in terms of the evolution of the electronic orbital alignment from point to point on the intermediate excited-state potential-energy curve. The results, using model potentials for the metal-atom–rare-gas interaction, are in good agreement with the experimental polarization data.
[S1050-2947(98)00103-6]

PACS number(s): 33.70.−w, 34.10.+x, 34.50.Rk

The spectroscopy of the scattering states of a collisional molecule can give unique insight into molecular dynamics [1]. For example, the scattering of polarized light from a system of colliding atoms can be used to probe the dynamical evolution of the electronic orbital alignment through the collision [1–10]. A rigorous calculation of the polarized scattered light spectrum for the case of two colliding atoms has been given by Burnett and Cooper using a master-equation approach to derive the spectral correlation function [2,3]. A phenomenological solution, based on the intuitive orbital-locking and -following model [4,5] has also been developed to give qualitative insight into the molecular dynamics [6]. The depolarization of light scattered from the far wings of a collision broadened atomic spectral line can be interpreted in terms of the angular reorientation of the electronic orbital from the Franck-Condon point of excitation to separated products.

Havey and co-workers recently have used an experimental approach involving a two-color, two-photon absorption process within a single strong collision to probe the dynamics of electronic orbital following on a point-to-point scale within the collision. This approach, termed the ''fractional collision'' method, allows an investigation of the molecular dynamics on a subpicosecond time scale using frequency-resolved pump-probe techniques [7–9]. A formal theory for this process has been presented by Alber and Cooper [11]. Fractional collision experiments have been carried out by Olsgaard and co-workers on Mg-Ne and Mg-Ar systems [7–9]. The fractional collision process between the Mg atom and rare-gas perturber P can be described as (Fig. 1)

$$\mathrm{Mg}(3s^2)+P\rightarrow[\mathrm{Mg}P(3s^2\ {}^1\Sigma_0^+)], \tag{1a}$$

$$[\mathrm{Mg}P(3s^2\ {}^1\Sigma_0^+)]+\hbar\omega_{\mathrm{pump}} \rightarrow[\mathrm{Mg}P^*(3s3p\ {}^1\Pi_1\ \text{or}\ {}^1\Sigma_0^+)], \tag{1b}$$

$$[\mathrm{Mg}P^*(3s3p\ {}^1\Pi_1\ \text{or}\ {}^1\Sigma_0^+)]+\hbar\omega_{\mathrm{probe}} \rightarrow[\mathrm{Mg}P^{**}(3s5s\ {}^1\Sigma_0^+)], \tag{1c}$$

followed by

$$[\mathrm{Mg}P^{**}(3s5s\ {}^1\Sigma_0^+)]\rightarrow\mathrm{Mg}^{**}(5s)+P. \tag{1d}$$

In a quasimolecular picture, the Mg-P collision complex evolves adiabatically on the ground $[\mathrm{Mg}P(3s^2\ {}^1\Sigma_0^+)]$ electronic surface to R_1, the Franck-Condon point for a transition to the molecular excited states of character $\mathrm{Mg}P^*(3s3p\ {}^1\Pi_1$ or $\ {}^1\Sigma_0^+)$. The Condon point R_1 is determined by the frequency detuning of the pump laser from the $\mathrm{Mg}(3s^2\text{-}3s3p)$ resonance by

$$\hbar\Delta_1=\hbar(\omega_{\mathrm{pump}}-\omega_{3s\text{-}3p})=[V_{3p}(R_1)-V_{3s}(R_1)], \tag{2a}$$

where $V_i(R)$ is the collisional interaction energy for the ground state ($i=3s$) or the intermediate excited state ($i=3p$) of the MgP collisional molecule. This quasimolecular interpretation is expected to be valid in the far line wings such that $\Delta_1\tau_c\gg1$, where τ_c is the typical duration of strong collision (i.e., a collision occurring within the Weisskopf radius) [1,2,11].

The aligned atomic p orbital in the Mg-P collision complex is assumed to follow the rotating internuclear axis adiabatically through the collision to a second Franck-Condon

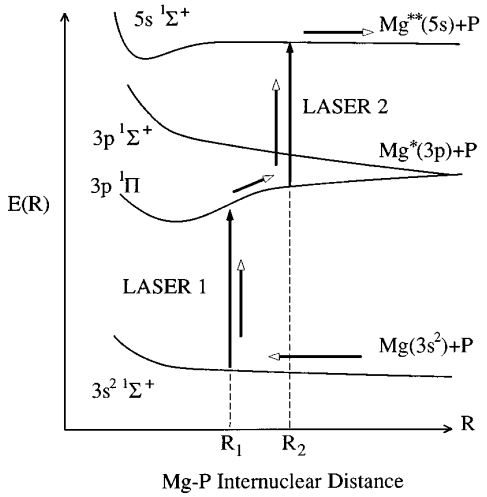

FIG. 1. Schematic potentials and pump-probe transitions in the fractional collision process.

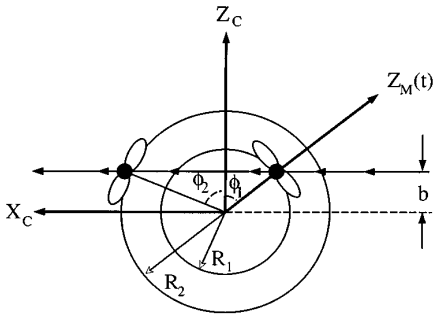

FIG. 2. Collisional geometry shown for the case of Π-state excitation and $R_1 < R_2$.

transition to a higher excited state MgP**$(5s\ ^1\Sigma_0^+)$ at R_2. The second Condon point is determined by the probe laser detuning

$$\hbar\Delta_2 = \hbar(\omega_{\text{probe}} - \omega_{3p\text{-}5s}) = [V_{5s}(R_2) - V_{3p}(R_2)]. \quad (2b)$$

The atomic cascade fluorescence from Mg**$(5s)$ serves as a measure of the two-photon excitation probability. In the quasimolecular picture, the experiment probes the evolution of the MgP collisional molecule along a portion of the collision trajectory (from R_1 to R_2) in the intermediate MgP*$(3p\ ^1\Pi_1$ or $3p\ ^1\Sigma_0^+)$ excited state.

Here we apply the orbital-locking and -following approach to the two-photon fractional collision problem and present a simple analytic solution for the polarization spectrum. A rigorous, quantitative comparison between experiment and theory is not possible due to the lack of accurate excited-state potential-energy curves. Furthermore, the fractional collision experiments of Olsgaard and co-workers were carried out at relatively small detunings for both pump and probe lasers so that $\Delta\tau_c \sim 1$ and the quasimolecular analysis may not be completely reliable [7–9]. Nevertheless, our model results show reasonable agreement with the experimental data over much of the spectrum and give a useful theoretical framework for interpreting the experimental polarization spectra in terms of the molecular-orbital reorientation on a point-to-point basis through the collision [8].

The theoretical model can be developed with reference to a set of three coordinate systems with coincident origins (Fig. 2). The space-fixed laboratory frame is defined by the laser polarization vector and the excitation and detection geometry in a standard mutually orthogonal arrangement. The space-fixed collision frame is oriented such that the collision trajectory lies in the X_c-Z_c plane. The collision frame is obtained from the laboratory frame by a rotation through Euler angles (ξ,η,ζ). Finally, we define a body-fixed molecular frame such that y_m lies along Y_c, and z_m lies along the instantaneous internuclear axis. The molecular and collision frames are related by a time-dependent rotation through the angle ϕ about the Y_c axis.

We first consider the case where the pump laser is detuned to the red of the Mg*$(3s\text{-}3p)$ resonance transition and assume that the radiative transition preferentially excites the attractive $^1\Pi$ state of the MgP collisional molecule. The Born-Oppenheimer electronic ground-state eigenfunction may be written $|3s\ ^1\Sigma^+(0)\rangle_{\text{MF}}$, referred to the molecular frame. The wave function evolves adiabatically on the ground-state potential to the first Condon point at R_1. In a Franck-Condon transition at R_1 (corresponding to rotation angle ϕ_1) the complex is pumped to the $3p\ ^1\Pi$ state of the complex. The excited-state wave function $|\Psi_p\rangle_{\text{MF}}$ can then be written as a linear combination

$$|\Psi_p\rangle_{\text{MF}} \propto \sum_{\Omega=\pm 1} |^1\Pi(\Omega)\rangle\langle^1\Pi(\Omega)|\boldsymbol{\varepsilon}_1\cdot\mathbf{r}|^1\Sigma^+(0)\rangle, \quad (3)$$

where ε_1 is the polarization vector of the first laser (the ''pump''), chosen to lie along the laboratory z axis, and $\mathbf{r}$ is the usual dipole operator.

We assume that the wave function and the electronic orbital alignment evolve adiabatically in the $^1\Pi$ state to the probe Condon point R_2 at rotation angle ϕ_2, where the complex is pumped in a second Franck-Condon transition to the higher state Mg$P(5s\ ^1\Sigma^+)$ [12]. The matrix element for the two-step radiative excitation can then be expressed as

$$M = \sum_{\Omega=\pm 1} \langle 5s\ ^1\Sigma^+|\boldsymbol{\varepsilon}_2\cdot\mathbf{r}|^1\Pi(\Omega)\rangle\langle^1\Pi(\Omega)|\boldsymbol{\varepsilon}_1\cdot\mathbf{r}|^1\Sigma^+(0)\rangle. \quad (4)$$

The dipole matrix elements can be evaluated by the Wigner-Eckart theorem to give

$$M = (\mathbf{r}_{3s\text{-}3p})(\mathbf{r}_{3p\text{-}5s}) \sum_{m,r,q} \sum_{\Omega=\pm 1} (\boldsymbol{\varepsilon}_2\cdot\boldsymbol{\varepsilon}^*_{-m}) D^{*(1)}_{0q}(\xi,\eta,\zeta) \times D^{(1)}_{mr}(\xi,\eta,\zeta) d^{(1)}_{q\Omega}(\pm\phi_1) d^{(1)}_{r\Omega}(-\phi_2), \quad (5)$$

where the $\mathbf{r}_{i-j}$ are the reduced dipole matrix elements for the respective atomic transitions, the rotation matrices give the projections of the laser polarization vectors onto the instantaneous transition dipole moment axes, and $\boldsymbol{\varepsilon}_2\cdot\boldsymbol{\varepsilon}^*_{-m}$ gives the projection of the probe laser polarization vector onto the space-fixed laboratory frame. The polarization-dependent signal intensity is then obtained by squaring Eq. (5) and averaging the over Euler angles ξ,η,ζ. The result depends primarily on the rotation angles ϕ_1 and ϕ_2.

In the Franck-Condon approximation and assuming a straight-line trajectory, ϕ_1 and ϕ_2 are determined by R_1 and R_2 and by the impact parameter b (Fig. 2). The final step in the calculation is an impact parameter average or, equivalently, an average over ϕ_1. R_1 and R_2 are determined by the detunings (Δ_1 and Δ_2) and the potential-energy curves $V_i(R)$ for the relevant quasimolecular states as in Eq. (2). Unfortunately, these states are not accurately known.

Malvern has carried out a model potential calculation for the ground and low-lying excited states of MgNe [13]. While the numerical precision is not adequate to allow a rigorous quantitative comparison with the experimental data, these theoretical curves can be used as a basis for a qualitative solution. We fit the long-range behavior of the theoretical potential-energy curves to simple analytic forms, which will allow a closed-form solution for the polarization spectrum.

The molecular states MgNe($3s^2\ ^1\Sigma^+$) and MgNe($3s3p\ ^1\Pi$) are assumed to be dominated by the long-range van der Waals interaction of the form $V_i(R) = -(C_i/R^6)(6)$ and the C_i coefficients are best fit values for the MgNe curves calculated by Malvern ($C_{3s}=50$ a.u. and $C_{3p}=175$ a.u.) [13]. The higher-lying MgNe($3s5s\ ^1\Sigma^+$) state is assumed to be essentially flat at long range, consistent with the model potentials.

We note that if R_1 is smaller than R_2, corresponding to $|\Delta_1|>|\Delta_2|$, the pump excitation step may occur either on the incoming or on the outgoing portion of the trajectory as shown in Fig. 2 and the impact parameter average yields an analytic result for the linear polarization P,

$$P=[15C^2+25C+50]/[9C^2+15C+90], \tag{6a}$$

where $C=[(C_{3p}-C_{3s})\Delta_2/(C_{5s}-C_{3p})\Delta_1]^{1/6}$. In this approximation P is a function of the van der Waals difference coefficients and the detuning of the two lasers alone. Furthermore, because of the weak dependence on the van der Waals coefficients, the calculated polarization is quite insensitive to the actual values of the fit parameters for the potential-energy curves.

If R_1 is larger than R_2, corresponding to the case $|\Delta_1|<|\Delta_2|$, then only the first Condon point (on the incoming portion of the trajectory) can contribute to the observed signal. In this case there is a maximum impact parameter and a maximum value for the angle ϕ_1, given by $(\phi_1)_{\max}=-\cos^{-1}(1/C)$. The averaging leads to a more complicated expression for the polarization,

$$P=\frac{[36C^2+60C+60-(36C+60-30/C+30/C^2+6/C^3)(C^2-1)^{1/2}]}{[12C^2+20C+220-(22C+20+216/C+10/C^2+2/C^3)(C^2-1)^{1/2}]}, \tag{6b}$$

with C defined as above.

The comparison of the theoretical calculation and the results for the MgNe and MgAr fractional collision experiments of Olsgaard *et al.* [8] are shown in Fig. 3(a). The experimental data have been obtained by a zero-pressure extrapolation in order to eliminate collisional depolarization effects as discussed in Ref. [8].

If the pump laser is detuned to the blue of the Mg($3s$-$3p$) resonance, the radiative excitation will be predominantly to the repulsive MgNe($3p\ ^1\Sigma^+$) state. To simplify the solution and develop a closed-form analytic solution, we assume the initial and final MgP($3s^2\ ^1\Sigma^+$ and $3s5s\ ^1\Sigma^+$) states to be flat and that the intermediate MgP($3s3p\ ^1\Sigma^+$) state can be approximated by an exponential form $V_\Sigma(R)=Ae^{-BR}$ ($A=0.154$ a.u. and $B=0.432$ a.u.). These assumptions are in qualitative agreement with the model potentials [13]. As in the preceding discussion, the polarization results are relatively insensitive to the potential fit parameters in any case.

Proceeding as before, we can evaluate the linear polarization for the case $R_1<R_2$ as

$$P=9C^2/[25+3C^2] \tag{7a}$$

and for the case $R_2<R_1$ as

$$P=\frac{18C^2+(3C^3-45C+12/C)(C^2-1)^{1/2}}{6C^2+50+(-9C^3+3C-44/C+26/C^3)(C^2-1)^{1/2}}, \tag{7b}$$

where $C=[\ln(|A/\Delta_1|)/\ln(|A/\Delta_2|)]$ [13].

The polarization results are compared with the available experimental data for MgAr in Fig. 3(b). In this blue wing detuning case there are few MgNe data reported in Ref. [8] for comparison. In addition, for MgAr, no zero-pressure extrapolation to the experimental data is available. Data are reported are pressures of 10 and 50 Torr, so that there will be some effect due to collisional depolarization in the experimental results.

In the experimental polarization spectrum reported in Ref. [8], there is a resonance peak where the polarization approaches $P=100\%$. This resonance occurs at the probe detuning $\Delta_2=-\Delta_1$, corresponding to the two-color, two-photon $3s^2$-$3s5s$ transition in the isolated Mg atom. This atomic process is unrelated to the collisional processes of interest here; the feature is present for any (or no) buffer gas. In Fig. 3 the two-photon atomic resonance position is marked by a vertical line. There is a second resonance in the intensity spectrum at $\Delta_2=0$, corresponding to the isolated Mg($3s3p$-$3s5s$) atomic transition. In this work we are interested in transitions in the quasimolecular regime, corresponding to pump-probe excitation of the MgP collisional molecule. Thus the experimental data in the region of the atomic resonance transitions has been omitted for clarity.

The orbital-locking and -following model explains the weak variation in the polarization spectrum in terms of the rotation of the electronic p orbital through the collision [4–6]. While simplistic, this model does give reasonable agreement with the experimental results. The predictions are in good qualitative agreement with the experimental data, approximately reproducing the correct polarization sign and magnitude, and the weak dependences on probe laser detuning in the quasimolecular regime.

Agreement in the case of Π-state excitation ($\Delta_1=-25.5\ \mathrm{cm}^{-1}$) is quite good [Fig. 3(a)], showing a strong polarization asymmetry about the two-photon resonance position ($\Delta_2=+25.5\ \mathrm{cm}^{-1}$). The polarization in the region $0<\Delta_2<-\Delta_1$ is moderate and increases slowly with probe detuning Δ_2. In this regime $R_1<R_2$ and as the detuning increases, the probe point (R_2) moves in to a smaller internuclear distance, approaching the pump point (R_1). This corresponds to a decreasing degree of orbital reorientation and the observed polarization subsequently increases. For detunings Δ_2 larger than $-\Delta_1$, corresponding to the regime $R_2>R_1$, the theory predicts a very high (and roughly flat) positive polarization, in reasonable agreement with experimental results.

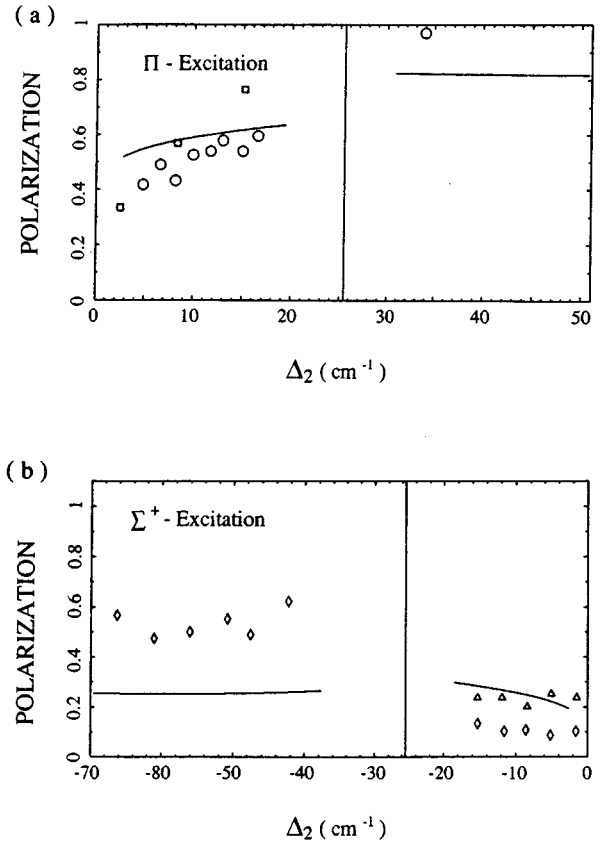

FIG. 3. (a) Mg rare-gas fractional collision polarization spectra for $\Delta_1 = -25.5\ \mathrm{cm}^{-1}$, corresponding to the case of Π-state excitation. The theoretical calculation is indicated by the solid line. Experimental results are the zero-pressure limit data taken from Ref. [8] and are shown as open circles for Mg-Ne and open squares for Mg-Ar. (b) Mg rare-gas fractional collision polarization spectra for $\Delta_1 = +25.5\ \mathrm{cm}^{-1}$, corresponding to Σ^+-state excitation. The theoretical calculation is indicated by the solid line. Experimental results are taken from Ref. [8] and are shown as open triangles (10 Torr) and open diamonds (50 Torr).

The agreement between experiment and theory is also good in the case of Σ^+-state excitation ($\Delta_1 = +25.5\ \mathrm{cm}^{-1}$), at least for $-\Delta_1 < \Delta_2 < 0$ [Fig. 3(b)]. In this detuning range the polarization is relatively low and increases with probe detuning toward the two-photon atomic resonance. Note in this region the collisional depolarization effect apparent in the difference between the 10- and 50-Torr MgAr data. The predicted polarization is in very good agreement with the lower-pressure data.

The most significant discrepancy occurs in the regime $\Delta_2 < -\Delta_1$, where the observed polarization is significantly larger than that predicted by this simple theoretical model. Note that the data in this regime are all taken at higher pressures and so eliminating the systematic collisional depolarization would serve to make this disagreement between the experimental results and the model predictions even more significant. The specific reasons for this discrepancy are not clear, but it should be noted that the crude approximations we have made for the shape of the Mg$P^*(3s3p\ ^1\Sigma^+)$ and Mg$P^{**}(3s5s\ ^1\Sigma^+)$ potential-energy curves (based on the model potentials for MgNe) may not be appropriate for the MgAr system. Trajectory effects (involving the breakdown of the impact parameter approximation) may be more important for this detuning case. Finally, the experiments of Olsgaard and co-workers [8] are carried out at relatively small detunings so that the quasimolecular interpretation may not be strictly valid. The the calculation neglects any contribution from direct two-photon excitation processes that can be important at these small detunings. These direct two-photon contributions (including the effect of quantum interference with the indirect pathways) are likely to be important under these small-detuning experimental conditions [11].

While this model is simplistic, it is yet (to the best of our knowledge) the only model prediction for the experimental polarization spectrum reported by Olsgaard and co-workers [8]. The calculation can be made more accurate and reliable by using better potential-energy curves and choosing more realistic trajectories. The contributions from direct two-photon excitation processes (and the interference between these competing pathways) could also be included as discussed in Ref. [11]. This might allow a sensitive and quantitative test of the orbital-following approximation on a point-to-point scale through the collision. Of course, we would then lose the advantage of a simple closed-form analytic solution for the polarization spectrum and much of the qualitative insight into the orbital reorientation dynamics it allows.

The authors gratefully acknowledge helpful discussions with Professor Mark Havey. This work was supported by the National Science Foundation.

[1] P. D. Kleiber, in *The Chemical Dynamics and Kinetics of Small Radicals*, edited by K. Liu and A. Wagner (World Scientific, Singapore, 1995), p. 573.
[2] K. Burnett, Phys. Rep. **118**, 339 (1985).
[3] K. Burnett *et al.*, Phys. Rev. A **22**, 2005 (1980); K. Burnett and J. Cooper, *ibid.* **22**, 2027 (1980); **22**, 2044 (1980).
[4] J. Grosser, Z. Phys. B **14**, 1449 (1981).
[5] E. E. B. Campbell *et al.*, Adv. Chem. Phys. **72**, 37 (1988).
[6] E. L. Lewis *et al.*, J. Phys. B **14**, L173 (1981); E. L. Lewis *et al.*, *ibid.* **16**, 553 (1983).
[7] D. A. Olsgaard *et al.*, Phys. Rev. A **43**, 6117 (1991); D. A. Olsgaard *et al.*, Phys. Rev. Lett. **69**, 1745 (1992).
[8] D. A. Olsgaard *et al.*, Phys. Rev. A **48**, 1987 (1993).
[9] R. A. Lasell *et al.*, Phys. Rev. A **50**, 423 (1994).
[10] S. Ananthamurthy and P. D. Kleiber, J. Chem. Phys. **102**, 1917 (1995).
[11] G. Alber and J. Cooper, Phys. Rev. A **31**, 3644 (1985).
[12] In the orbital-locking and -following model, a locking radius R_L is assumed, beyond which the orbital no longer follows the molecular axis but remains space fixed. If $R_L < R_2$ we should properly use a locking radius to define the point where the excited-state orbital becomes space fixed. All of results given would be the same with the replacement $R_2 \rightarrow R_1$.
[13] A. R. Malvern, J. Phys. B **11**, 831 (1978).